The Holocene
http://hol.sagepub.com/

# Connecting the Atlantic-sector and the north Pacific (Mt Logan) ice core stable isotope records during the Holocene: The role of El Niño

David A. Fisher

*The Holocene* 2011 21: 1117 originally published online 18 July 2011
DOI: 10.1177/0959683611400465

The online version of this article can be found at:
http://hol.sagepub.com/content/21/7/1117

Published by:
SAGE
http://www.sagepublications.com

**Additional services and information for *The Holocene* can be found at:**

**Email Alerts:** http://hol.sagepub.com/cgi/alerts

**Subscriptions:** http://hol.sagepub.com/subscriptions

**Reprints:** http://www.sagepub.com/journalsReprints.nav

**Permissions:** http://www.sagepub.com/journalsPermissions.nav

**Citations:** http://hol.sagepub.com/content/21/7/1117.refs.html

>> Version of Record - Sep 28, 2011

OnlineFirst Version of Record - Jul 18, 2011

What is This?

Downloaded from hol.sagepub.com at Masarykova Univerzita on April 4, 2013

*Research paper*

The Holocene
21(7) 1117–1124
© The Author(s) 2011
Reprints and permission:
sagepub.co.uk/journalsPermissions.nav
DOI: 10.1177/0959683611400465
hol.sagepub.com
SAGE

# Connecting the Atlantic-sector and the north Pacific (Mt Logan) ice core stable isotope records during the Holocene: The role of El Niño

**David A. Fisher**
Department of Earth Sciences, University of Ottawa, Canada, and Geological Survey of Canada, NRCan, Canada

**Abstract**
The $\delta(^{18}O)$ Holocene of the Mt Logan ice core is very different from those of eastern Arctic Canada and Greenland. The large changes seen in Logan dwarf even the largest change (the cooling event 8200 years ago) in the Atlantic-sector cores. Large changes in Logan's $\delta(^{18}O)$ and d are related to the state of El Niño as reflected by the Quelccaya $\delta(^{18}O)$ series. It is found that the lagged auto-difference series of the ice core records from the Agassiz ice cap, Greenland and the 23-site stack of paleotemperature records of Kaufman et al. (Kaufman DS, Schneider DP, McKay NP, Ammann CM, Bradley RS, Briffa KR et al. (2009) Recent warming reverses long-term Arctic cooling. *Science* 325: 1236) produce highly significant matches to the Mt Logan $\delta(^{18}O)$ series. These correspondences suggest a lag of 1200 years. This lag time is what some models of the Diffusive-Great Ocean Conveyor (D-GOC) predict for the average travel time from the North Atlantic to the tropical eastern Pacific. Monte Carlo testing of the correlations show that they are very significant. The implications of ENSO being affected by the difference between temperatures today and those of 1200 years ago are touched on.

**Keywords**
Agassiz, El Niño, Great Ocean Conveyor, Greenland, Holocene, ice cores, La Niña, Mt Logan, stable isotopes

## Introduction and plan

The $\delta(^{18}O)$ Holocene history from ice cores, lakes and peat inception dates that are taken close to the north Pacific do not look like those from Greenland or eastern Arctic Canada (Fisher et al., 2004, 2008). In particular, the Holocene $\delta(^{18}O)$ record from the 5400 m a.s.l. site on Mt Logan differs greatly from the North Atlantic ice cores. See for example Figure 1, which compares the Mt Logan $\delta(^{18}O)$ record to that of Renland/Agassiz (Vinther et al., 2009). It has been proposed that the Logan record's large $\delta(^{18}O)$ and d (deuterium excess) changes are caused by shifts in the source regions for the moisture (Fisher et al., 2008, 2004). Such large changes cannot reflect large temperature changes because of their size and non-synchronicity with the Atlantic cores.

This paper will argue that the Mt Logan $\delta(^{18}O)$ is largely driven by the strength of El Niño, which in turn is determined by the present tropical Pacific climate and that of 1200 years ago in the North Atlantic via the Diffusive-Great Ocean Conveyor (D-GOC) (Broecker, 1991; Holzer and Primeau, 2006). The Holocene temperature histories are taken as those given by the Holocene ice core records from Greenland, Arctic Canada (Vinther et al., 2009) and, for the most recent 2000 years, by the 23-Arctic-site multiproxy stack of Kaufman et al. (2009).

The ice core $\delta(^{18}O)$ Holocene records from the Greenland ice sheet reflect the history of air temperature plus ice-thickness change, while the surrounding smaller ice caps on Renland (east Greenland) and Agassiz (northern Ellesmere Island, Canada) show the Holocene temperature record (Vinther et al., 2008, 2009). There is now a consensus that the early Holocene of the North Atlantic region had a thermal maximum about 8500 to 10 000 years ago and has cooled about 3°C since (Fisher and Koerner, 2003; Vinther et al., 2009). We shall refer to the records from the eastern Canadian Arctic, Greenland and the Kaufman et al. 2000-year record as North Atlantic records and the Logan $\delta(^{18}O)$ as a Pacific record.

The recent stacks of La Niña and El Niño proxy series reported in Gergis and Fowler (2009) are taken as the best measure of their strength over the last 500 years. As previously pointed out, the Quelccaya ice core $\delta(^{18}O)$ series (Thompson et al., 1984) is well correlated to El Niño, Figure 2. The stacked Quelccaya $\delta(^{18}O)$ series go back over 1000 years and are taken as a proxy for El Niño.

The simple model of Sun (2000) characterizes the chaotic oscillation between La Niña and El Niño using the tropical Pacific's warm pool temperature $T_w$, the water temperatures under the mixed layer (at a few hundred meters depth), $T_c$, and the thickness of the tropical mixed layer, $h$. The main driver of the Sun model is the temperature difference ($T_w - T_c$), Figure 3. Several

Received 20 July 2010; revised manuscript accepted 15 December 2010

**Corresponding author:**
David A. Fisher, GSC-NRCan Glaciology, University of Ottawa, Earth Sciences, 601 Booth Street, 3rd Floor, Ottawa K1A 0E8, Canada.
Email: fisher@nrcan.gc.ca

Downloaded from hol.sagepub.com at Masarykova Univerzita on April 4, 2013

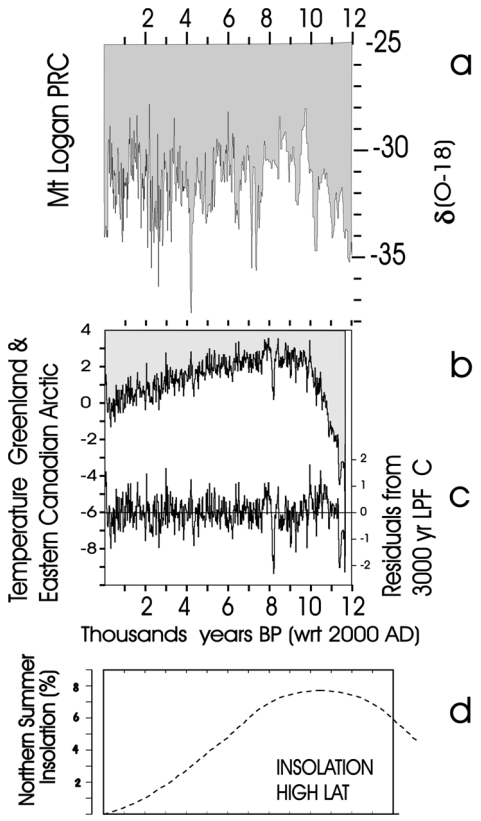


**Figure 1.** Comparing the Logan δ($^{18}$O) record to the Holocene proxy temperature record derived for Greenland and eastern Arctic Canada (Vinther et al., 2009). (a) The Logan δ($^{18}$O) record (Fisher et al., 2008). Using the conversion factor from (Vinther et al., 2009) of 0.48‰/°C shows this δ($^{18}$O) record can not be a temperature history, because the inferred changes would be much too large and out of phase with (b). (b) The stacked Greenland and eastern Canadian Arctic proxy temperature record from Vinther et al. (2009). (c) Residuals from a 3000-year low pass filtering of the (b) series. (d) Summer insolation at latitude 75°N (Laskar, 1990). Modern July insolation is 457 W/m$^2$ at 60°N (Berger and Loutre, 1991) and the January insolation is only 37 W/m$^2$. By far most of the annual radiation budget is driven by the summers, because winter has so little insolation. In the tropics by contrast there is relatively little seasonal difference and the annual insolation is rather constant through the Holocene

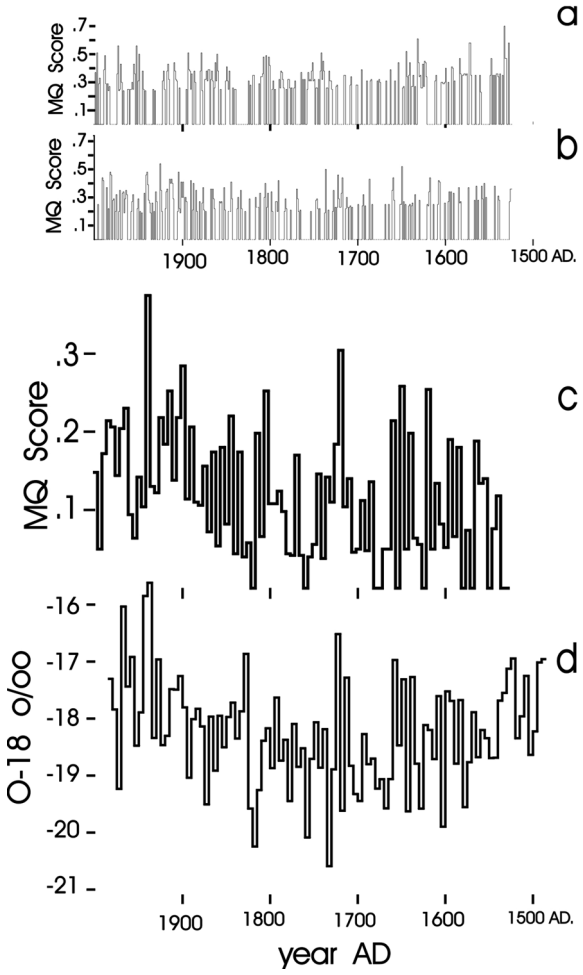


**Figure 2.** Stack of La Niña and El Niño strength proxies (Gergis and Fowler, 2009) based on 15 proxy records. (a) MQ scores for La Niña. (b) MQ scores for El Niño. (c) Five-year averages of El Niño MQ scores. (d) Five-year averages of the two Quelccaya δ($^{18}$O) series (Thompson, 1992; Thompson et al., 1984)

Atlantic-sector Holocene temperature proxy series, $T_s(t)$, are used to estimate $T_w$. It is further assumed that $T_c$ can be estimated from $T_s$ ($t$-lag), where 'lag' is the time it takes for changes in the North Atlantic's temperature (and salinity) to travel by a D-GOC (Broecker, 1991) to the eastern tropical Pacific near the surface (Holzer and Primeau, 2006).

The Logan δ($^{18}$O) Holocene record is correlated with [$T_s$ ($t$) − $T_s$($t$-lag)] over a range of lags from 50 to 2500 years and the lag of about 1200 years gives the highest correlation using three proxy estimators $T_s$ ($t$). When the melt layer percentage from the Agassiz ice cap is used for $T_s$ ($t$), see Figure 6b, a Monte Carlo analysis shows the maximum correlation is significant at the 99.7% level, see Figure 7. This approximate 1200-year lag time shows up in a number of ocean-ballasted models (Holzer and Primeau, 2006; Stocker and Johnsen, 2003).

This paper addresses the question: Can one relate the (ice core) Holocene records of Greenland and Arctic Canada to Mt Logan's? Tentatively, the answer is 'yes'.

## Proxy records for La Niña and El Niño and Logan δ($^{18}$O)

The Logan ice core comes from the Mt Logan plateau 5400 m a.s.l. in the southwestern Yukon (Lat 60°N) and has been extensively reported in Fisher et al. (2004, 2008). Fisher et al. hypothesized that the very large shifts in the Logan δ($^{18}$O) and d (little d) time series are caused by switching the source waters between tropical and high latitudes. Local temperature changes cannot explain the very large shifts in stable isotopes, but model calculations suggest that they could be accomplished by switching between meridional and zonal water source flux. The model predicts that the size and sign of the isotope changes is a function of elevation. The switching is associated with the strength of El Niño. During times of weak El Niño and steady La Niña, Logan water sources tend to be from high latitudes. When El Niño is strong and frequent, there is stronger meridional water vapour flow from the tropics to the high-elevation Logan site (Moore et al., 2001, 2005). The Fisher-model is a 'semi-empirical black box' that distributes source moisture by source, distance from source and elevation. Holdsworth's (2008a, b) model for δ($^{18}$O) of snow in high mountainous regions 'looks inside' the black box as does that of Field et al. (2010). So far, the only model that can

Downloaded from hol.sagepub.com at Masarykova Univerzita on April 4, 2013

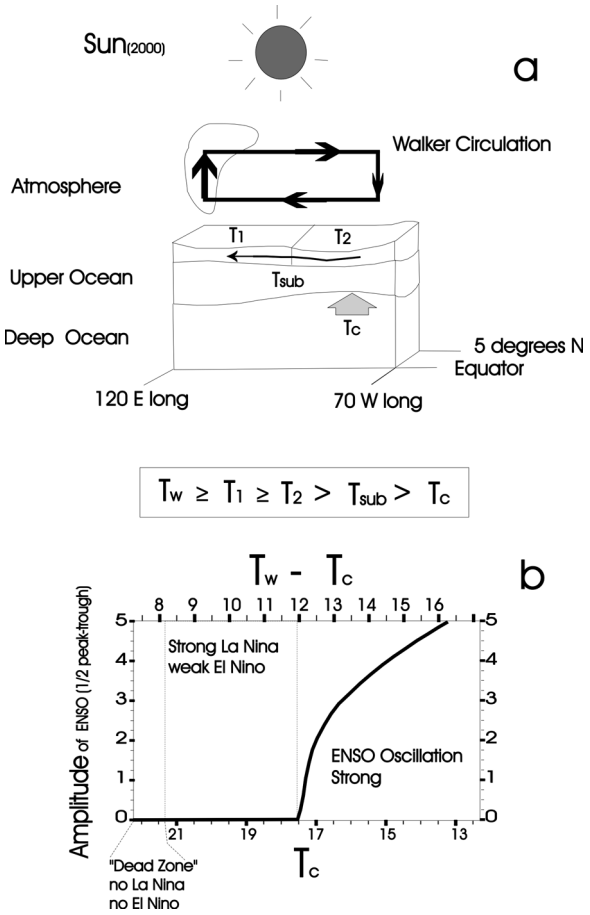


**Figure 3.** The Sun (2000) model's tropical Pacific that contains the ENSO instability. (a) The eastern Pacific has sea surface temperature (SST) $T_2$ and the western Pacific SST $T_1$. The 'warm pool' or maximum temperature for SSTs in the tropical Pacific ocean is denoted $T_w$. The easterly wind strengths that drive the surface currents are assumed proportional to the temperature difference ($T_1 - T_2$). The deeper colder ocean water with temperature $T_c$ is drawn upward by these easterly winds and changes the water temperature $T_{sub}$ just below the mixed surface layer. This upwelling in the TEP (tropical eastern Pacific) is part of the GOC (Holzer and Primeau, 2006). The various temperatures and their relative sizes are indicated in the figure. When the easterlies are strong, the rainfalls in the western Pacific are enhanced. (b) The Sun (2000) model solution map. The amplitude of the predicted ENSO 'oscillation' as a function of $T_c$. ENSO-like behavior starts very suddenly at $T_c$ = 17.5°C and the amplitude grows very fast as $T_c$ cools. $T_c$ is determined by the North Atlantic SST some time in the past via the GOC (Holzer and Primeau, 2006)

reproduce the size of δ($^{18}$O) changes and their elevation sensitivity is Fisher et al. (2004). But, for this discussion, the correctness of the Fisher et al. model is not critical.

While the Logan isotope record has a clear Younger Dryas and late glacial signature (Fisher et al., 2008), its Holocene does not resemble that of Greenland or Arctic Canada. Figure 1 illustrates the enormous differences between the Logan δ($^{18}$O) and what is now regarded as the temperature history of the North Atlantic as given by the ice cores of Greenland and Canada's eastern Arctic (Vinther et al., 2009).

The Mt Logan δ($^{18}$O) record has been previously compared to the 'documentary' Quinn et al. (1987) 450-year record of El Niño. But there are many documentary and proxy records of La Niña and El Niño (D'Arrigo et al., 2005; Fowler, 2008; Gergis, 2006; Mann et al., 2000; Quinn and Neal, 1992). Recently, Gergis and Fowler (2009) have compiled an average ENSO history using 15 documentary and proxy series. They made magnitude series of both La Niña and El Niño. When various records agreed there was a large event, its resulting magnitude was greater than if there was no unanimity amongst the records. In this even-handed way, they produced an annual time series of both phenomena. Figure 2a and b shows the two Gergis and Fowler (2009) annual series of 'MQ" (minimum adjusted magnitude score) values for La Niña and El Niño. Five-year averages of the El Niño series appear in Figure 2c, and Figure 2d shows the average of the two Quelccaya δ($^{18}$O) series (Thompson, 1992; Thompson et al., 1984). The El Niño and Quelccaya δ($^{18}$O) five-year average series have a correlation coefficient of 0.58 and thus the millennium-long Quelccaya stacked series is taken as a good proxy for El Niño.

## Summary of the Sun Model for the state and amplitude of ENSO

Sun has summarized his model of ENSO in a useful overview article (Sun, 2000). The variables in the Sun model are shown in Figure 3a and the 'amplitude' of the chaotic temperature oscillation produced by the model appears in Figure 3b. The half difference between the warm phase (El Niño) and the cold (La Niña) is determined by the temperature difference ($T_w - T_c$ ) between the warm pool and deeper ocean water. Sun's $T_c$ is a representative water temperature under the mixed layer at a depth of order 100 m. If the deeper water is too warm ($T_c$ > 17.5°C) then the ENSO amplitude is zero and the model predicts a constant strong La Niña. If $T_c$ is greater than 21.5°C, the model suggests there is zero ENSO amplitude with both El Niño and La Niña being very weak.

The main driver that pushes the solutions into the oscillatory-ENSO part of the map (Figure 3b) is $T_c$ becoming sufficiently cold. Sun (2000) suggests that the ENSO-type solution became possible about 5000 years ago, when $T_c$ cooled down enough, because the surface waters of the North Atlantic had finally cooled enough, see Figure 1d. While it is true the early-Holocene Pacific experiences few intervals with strong El Niños (because of the high latitude insolation maximum) there are early-Holocene cold excursions (e.g. between 8000 and 9000 BP) that work against this general trend and would result in episodes of oscillation, see Figure 1c. $T_c$ water is delivered slowly via the GOC (Broecker, 1991) or thermohaline process, which has its main subsidence-cooling zones at the high latitudes of the North Atlantic (Holzer and Primeau, 2006). In the early Holocene, these high latitudes were considerably warmer and fresher, because of the insolation maximum (Figure 1d). The Pacific tropical SST, $T_w$, is driven by the effects of sun, volcanic veils and internal feedbacks. $T_c$ is also driven by these same factors plus high-latitude summer insolation, all lagged to some extent, because it takes some lag time (mass flux average) for the sinking surface waters in the North Atlantic to travel the GOC and reach the near surface of the tropical eastern Pacific. Holzer and Primeau (2006) have modeled this travel time and suggest it is in fact a distribution whose flux average is about 1200 years. The GOC would be expected to make $T_c$ into a diffused version of the North Atlantic temperature history. But the very sharp response function defining the ENSO amplitude in Figure 3b could recapture some of the higher frequencies of the North Atlantic record.

Excluding the insolation, the high-latitude proxy temperatures ($T_s$) are affected by the same list of factors that drive $T_w$, thus it

Downloaded from hol.sagepub.com at Masarykova Univerzita on April 4, 2013

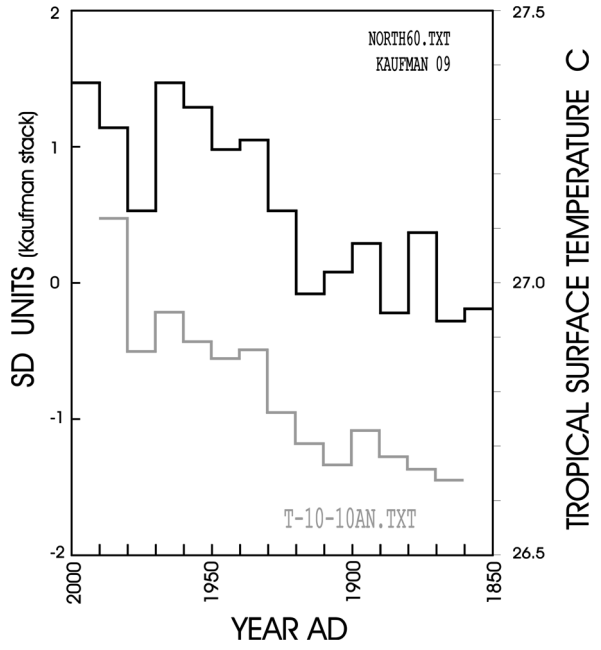


**Figure 4.** Decadal averages of the recent 150 years of the Kaufman et al. (2009) multiproxy temperature series in black, and the tropical temperatures (10°S to 10°N) in grey (Climate Research Unit, 1992). The proxy stack from 23 high-latitude sites has a correlation coefficient of 0.84 (5 d.f.) with the measured tropical temperatures

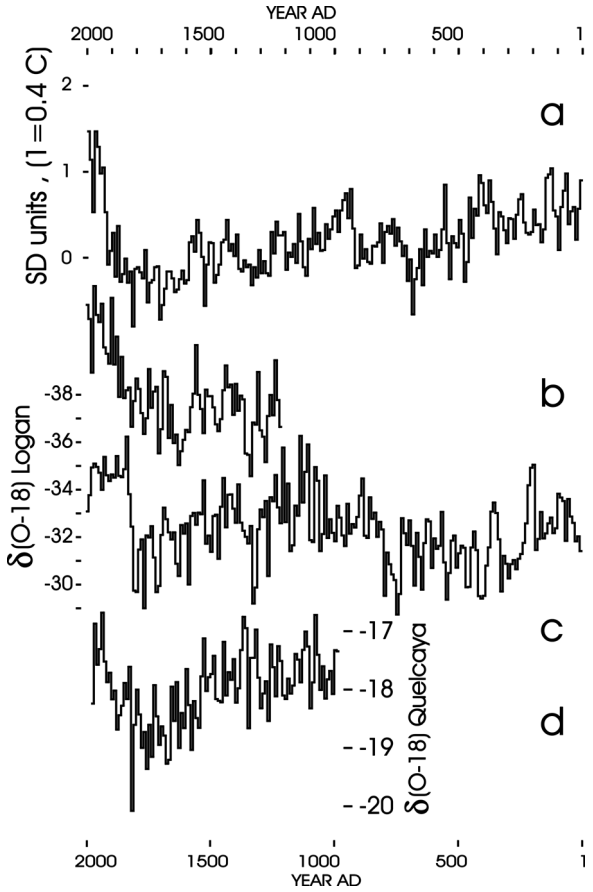


**Figure 5.** The last two millennia. (a) The Kaufman et al. (2009) multiproxy high latitude Northern temperature record. (b) The lagged difference series of the Kaufman stack, with a lag of 1210 years. (c) Decadal averages of the Mt Logan $\delta(^{18}O)$ record (Fisher et al., 2008). (d) Decadal averages of the Quelccaya $\delta(^{18}O)$ records (Thompson, 1992; Thompson et al., 1984)

will be assumed that the history of $T_w$ $(t)$ is proportional to $T_s(t)$, the temperature derived from the proxy records, but with some of the secular (high-latitude) insolation trend removed. For example, Figure 4 shows the most recent 150 years from the 23-site-stack of proxy Arctic temperatures (Kaufman et al., 2009) plotted against tropical (−10<latitude<10) temperatures (Climate Research Unit, 1992). The Kaufman et al. proxy has a correlation coefficient of 0.84 (d.f. = 5,5) with the measured tropical decadal averages. Furthermore $T_c$ will be estimated by the lagged record $T_s(t\text{-lag})$. As will be shown later, a lag of about 1200 years gives the best results. This lag was found previously and independently by Stocker and Johnsen (2003) as the best lag for generating Antarctic ice core isotope time series from those of Greenland during the Ice Age. Holzer and Primeau (2006) suggested that the GOC is not a mechanistic tube or current connecting the surface of the North Atlantic to that of the tropical eastern Pacific (TEP) in about 400 years travel time, but rather a pathway made diffusive in nature by eddies. Their ocean modeling finds the distribution of travel times weighted by delivered flux at the TEP is centered at about 1200 years. With the above assumptions:

$$T_w - T_c = \Delta T = \text{function}\,[T_s(t) - T_s(t\text{-lag})] \quad (1)$$

If Logan records El Niño/La Niña through its isotopes as suggested in Fisher et al. (2004, 2008), and if the $(T_w - T_c)$ time series can be estimated by high-latitude Atlantic-sector lagged difference series, Eq. (1), then the Logan isotope record [$\delta(^{18}O)$ and/or little d] should relate to $[T_s(t) - T_s(t\text{-lag})]$.

## The data sets

The target series to match is the Mt Logan $\delta(^{18}O)$ and/or d (deuterium excess) series. The time scale for the Mt Logan core (Fisher et al., 2008) is based on layer counting (upper 300 years), identified volcanic horizons (corroborated by tephra fingerprinting back to about 1645 BC (Froese et al., 2010)) and the end of the Younger Dryas (given the 9703 BC age from the GICC05 timescale (Vinther et al., 2008)). There are corroborated fixed points in the age model at AD 1700, AD 1516, AD 803, 1645 BC and 9703 BC. There are many other large volcanic(sulfate) horizons that can be plausibly identified with large eruptions in Alaska, the Aleution Islands and Kamkatka region (Fisher et al., 2008) or to episodes of early-Holocene volcanism (Zielinski et al., 1997). A smooth fit is run through the fixed points using a glaciological age model (Fisher et al., 2008). The timescale error at fixed points is as good as the dating for the fixed points. For interpolated-points between fixed points the error is up to ±5% of the time-distance from the closest fixed point. For example, the error in the 6000 BP age would be about ±120 years because of the fixed point at 3645 BP.

The driver series that will be used to match the Logan series will be: (1) the Kaufman 2000-year multiproxy series of temperature (Kaufman et al., 2009), (2) the Agassiz Holocene melt layer stack (Fisher et al., 1995) and (3) the Holocene ice core isotope series from the Canadian Arctic and Greenland (Vinther et al., 2009).

Kaufman et al.'s (2009) multiproxy temperature series based on 23 high-latitude series appears (10-year averages) in Figure 5a.

The Agassiz and Renland cores have been tied together and aligned with the canonical Greenland GIC005 timescale (Greenland Ice-Core timescale version 5) for the Holocene

Downloaded from hol.sagepub.com at Masarykova Univerzita on April 4, 2013

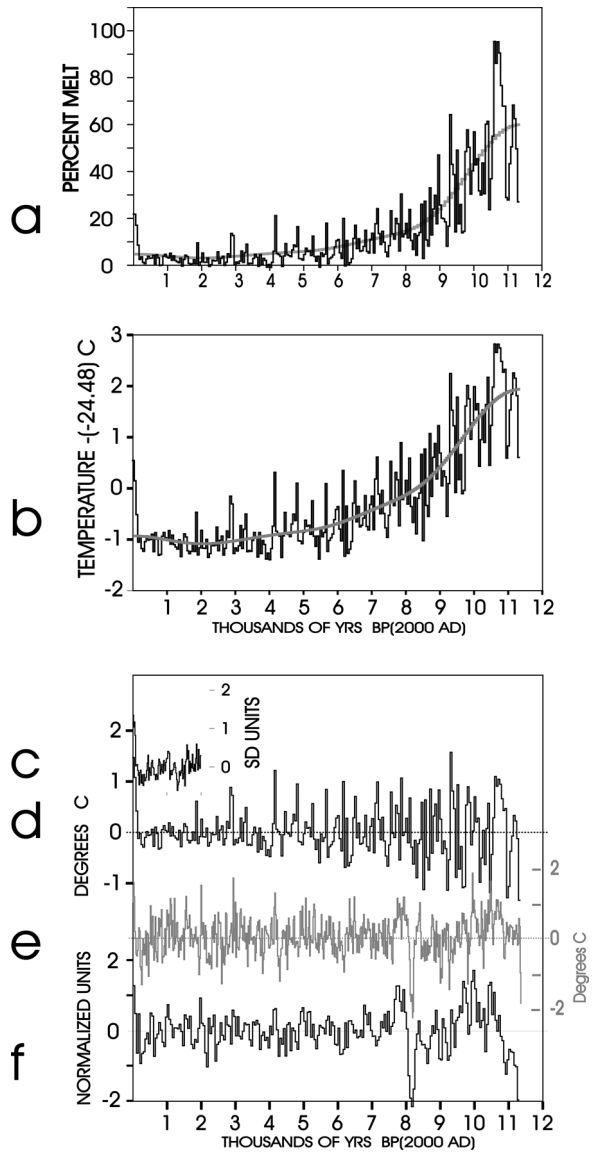


**Figure 6.** Melt layer record from Agassiz A84+A87, and residuals of melt and isotopes from a low pass filter (LPF). (a) Agassiz melt percentage A84+A87 and the 3000-year LPF through it. (b) Agassiz proxy temperatures derived from melt, using the calibration curve (Figure A1) in the Supplementary Material 1 (available online). (c) The residuals from a least squares line of the Kaufman et al. (2009) temperature proxy. (d) The residuals of proxy melt-derived temperatures. (e) A repeat of Figure 1c showing residual temperatures from the Holocene temperatures (Vinther et al., 2009). (f) The stack of the normalized residuals from $\delta(^{18}O)$ series from Renland+GRIP+GISP2+NGRIP+Agassiz A84+A87, six series in all (Vinther et al., 2008)

(Vinther et al., 2008). The Atlantic-sector Holocene $\delta(^{18}O)$-based temperature curve is presented in Figure 1b (Vinther et al., 2009).

The two adjacent Agassiz cores (about 100 m apart) at the top of the flow line A84 and A87 have similar records for $\delta(^{18}O)$ and melt (Fisher, 1988; Fisher et al., 1995; Koerner and Fisher, 1990). Their records are stacked to reduce noise. The stacked melt layer record and derived paleotemperature history for A84 and A87 are shown in Figure 6a, b. The melt percentage was converted to a proxy temperature (see supplementary material Figure A1, available online). Figure 6a,b smooth curves are from a 3000-year low pass filter (LPF) and the temperature residuals are shown in Figure 6d. Figure 6e repeats the temperature residuals from the Vinther et al. (2009) Holocene reconstruction (Figure 1c). Figure 6f shows the stacked and normalized residuals from $\delta(^{18}O)$ series from Renland, GRIP, GISP2, NGRIP, Agassiz A84 and A87. Figure 6c repeats the 2000-year Kaufman series residuals. There is clearly a high degree of coherence between all the residual series in Figure 6. The same approach and argument will be used for each of the types of driver series. For the Holocene, the melt series has an intuitively stable transfer function, i.e. the melting point of ice is constant, whereas the stable isotope transfer function can be complicated by storm track path and moisture source changes (Fisher, 1990, 1992; Johnsen et al., 1989).

## Scanning for maximum correlation

### *Using the Kaufman 2000-year series as a driver*

For this driver, Eq. (1) is reduced to

$$T_w - T_c = \Delta T = T_s(t) - T_s(t\text{-lag}) \quad (2)$$

where $T_s(t)$ are the 200 ten-year average values of the Kaufman series, shown in Figure 5a. Ten-year averages of the Logan $\delta(^{18}O)$ target series are shown in Figure 5c. The correlation coefficient between the Logan $\delta(^{18}O)$ and lagged differences of the Kaufman stack appear in Figure 7a. The largest (negative) correlation (−0.51) occurs when the lag equals 1210 years. Of course, the $(T_s(t) - T_s(t\text{-lag}))$ series gets shorter as the lag gets longer so the proper significance test for the 1210-year maximum is not possible. This problem, however, does not occur when the driver series are Holocene-long. The $(T_s(t) - T_s(t\text{-lag}))$ series for a lag of 1210 years is shown in Figure 5b just above the Logan $\delta(^{18}O)$ series. The fit with Logan is good. The Quelccaya $\delta(^{18}O)$ stack (El Niño proxy) appears in Figure 5d.

### *Using the Holocene melt and isotope driver series*

The big (insolation) trend from the early Holocene to the present will be partitioned from the series using a 3000 a LPF and treated separately from the residuals. The insolation trend is highly latitude sensitive (Laskar, 1990). The residuals left behind (periods less than about 3000 years) are assumed to be due to a mixture of solar and volcanic variations, readjustments from ice age loading and ocean responses.

Inspection of Figure 6d, e and f reveals that the residuals of temperature-melt and isotopes are significantly correlated (i.e. Figure 6d and f correlate at 0.29 for 100-year averages) and there is good cross-spectral phase agreement between them.

The Holocene driver series LPF part is denoted as $T_{sf}(t)$ and the residuals as $T_{sr}(t)$. The paleotemperature $T_s(t)$ can thus can be written as a function of time $t$:

$$T_s(t) = T_{sr}(t) + T_{sf}(t) \quad (3)$$

In order to keep the significance testing model simple and stringent, the lagged difference series is used based only on the residuals, namely:

$$\Delta T = T_{sr}(t) - T_{sr}(t\text{-lag}) \quad (4)$$

Downloaded from hol.sagepub.com at Masarykova Univerzita on April 4, 2013

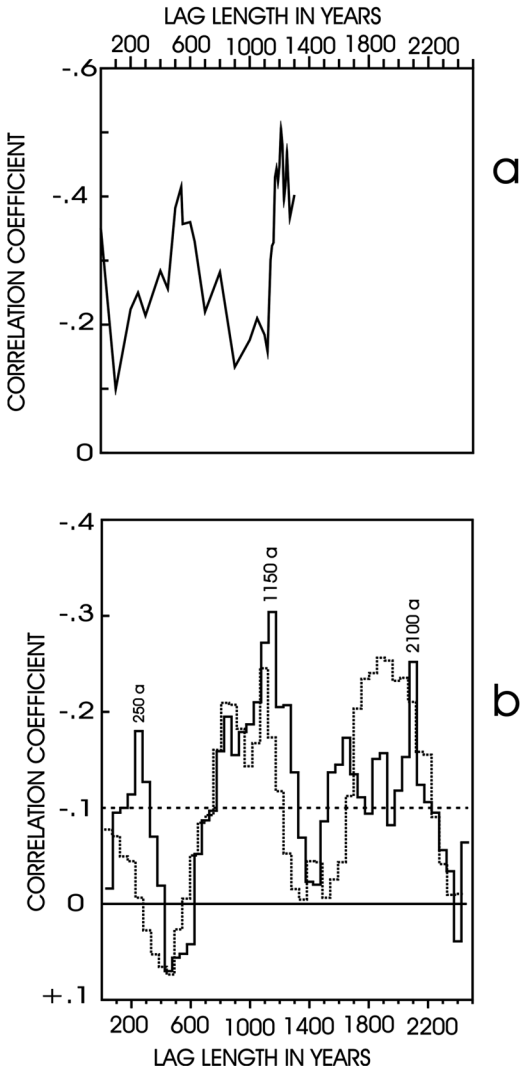


**Figure 7.** Correlation coefficients of lagged difference series with Mt Logan $\delta(^{18}O)$ vs. lag length. (a) The curve gives the correlation coefficient between the Logan $\delta(^{18}O)$ series and the lagged difference series using the Kaufman et al. (2009) multiproxy temperature series. The best correlation occurs for a lag of 1210 years. For lags greater than 1500 years, the correlations are not significant because the difference series get too short. (b) The solid line gives the correlation coefficient between the Logan $\delta(^{18}O)$ series and the lagged difference series using the residuals from the melt-derived temperatures. The largest (negative) correlation coefficient (−0.31) happens when the lag is 1150 years and it is significant at the 99.75% level. The dotted line shows the correlation between Logan $\delta(^{18}O)$ and the lagged difference series using the stacked residuals from all the $\delta(^{18}O)$ series, as shown in Figure 6f. While not as high, the peak correlation (−0.25) at lag 1100 years is still significant at the 95% level. The other maxima at lags of about 2000 to 2200 years are possibly a multiple of the 1150 peak

Note as described later, once the best lag time is found using the residuals the long-term secular trends and residual lagged series are recombined to produce the best estimate for the target series (see Appendix 2, available online).

If the Agassiz melt-layer temperature residual series of Figure 6d is used for $T_{sr}$ $(t)$ in Eq. (4), then the maximum (negative) correlation between $(T_{sr}$ $(t) - T_{sr}(t$-lag)) and the Logan $\delta(^{18}O)$ series is −0.31 for a lag of 1150 years. The correlation function is shown in Figure 7b (solid line) as a function of lag length. The significance of −0.31 was tested by generating 8000 (random) pseudo-driver series that had the same autocorrelations as the Agassiz melt-layer temperature residual series (i.e. 0.13 and 0.03), and differencing them with the whole range of lagged versions of themselves (lags 50 to 2500 years). It was found that a correlation coefficient of −0.31 is obtainable by chance only 20 times in 8000 realizations, which means it is significant at the 99.75% level (using a null test).

If the Holocene $T_{sr}$ $(t)$ driver series is derived from 50-year averages of six $\delta(^{18}O)$ residual series using all the Greenland and Agassiz records (Figure 6f), the correlation that the $(T_{sr}$ $(t) - T_{sr}$ $(t$-lag)) series makes with Logan $\delta(^{18}O)$ has a (negative) maximum of −0.25 at a lag of 1100 years, the dashed curve in Figure 7b. Monte Carlo tests show that chance could produce such correlations 5% of the time.

All the Arctic driver series maximize the correlation between $(T_{sr}$ $(t) - T_{sr}(t$-lag)) and Logan $\delta(^{18}O)$ when the lag is 1150 plus or minus 60 years. Note that the correlation functions shown in Figure 7b both have multiple maxima at about 1150 and about 2000 to 2200 years. It is possible that the larger is just double the smaller.

## Connecting the Logan $\delta(^{18}O)$ and d to the Agassiz paleotemperature

If, as suggested by Holzer and Primeau (2006), there is a range of possible travel times from 400 to 3500 years for water from the North Atlantic to reach the TEP, it would be more realistic to consider not just a simple single lagged series $(T_{sr}$ $(t) - T_{sr}(t$-lag)) but rather a weighted sum of lagged differences. Such a weighted lagged difference series expression is described in Appendix 2 (available online). Also described in Appendix 2 is the means by which the secular (filtered portion) of the Holocene driver series is included (that is, $f_1$ and $f_2$ are defined). Using a symmetric 1000-year-wide weighting function with a maximum at 1150 years, $f_1 = 0.4$ and $f_2 = 0.2$, the time series in Figure 8b is obtained. The travel time distribution of Holzer and Primeau (2006) weighted by flux contribution was also used as a source of weights, and the results were close to those shown below in Figure 8b. Figure 8c shows the Holocene Logan $\delta(^{18}O)$ isotopes, Figure 8d shows little d (deuterium excess) (Fisher et al., 2008) and Figure 8b shows the 'predicted' series using the Agassiz melt-temperature Holocene series whose residuals appear in Figure 8a.

It should be noted that the Agassiz melt-derived temperature trend line is likely too small in the interval 0 to 4000 years BP. As described in the supplementary material, this is due to the cold-end insensitivity of the calibration curve in Figure A1.

## Discussion and speculation

The ocean model work of Holzer and Primeau (2006) has shown that the GOC travel times between the North Atlantic subsidence zones and the upwelling zones in the tropical eastern Pacific are actually distributed over a wide range from about 400 to over 3000 years with a water-flux-weighted maximum at 1200 years, which is close to the lag times found from the ice core intercomparison studies.

Stocker and Johnsen (2003) derive a lag time of 1100 years by optimizing their model that connects the Greenland $\delta(^{18}O)$ Dansgaard/Oeschger events to their response features in Antarctic cores over 40 000 years ago. The D/O features have 'periods' of about 2000 years.

However, in this study, we are looking at higher-resolution Holocene variations. How are these finer details preserved from

Downloaded from hol.sagepub.com at Masarykova Univerzita on April 4, 2013

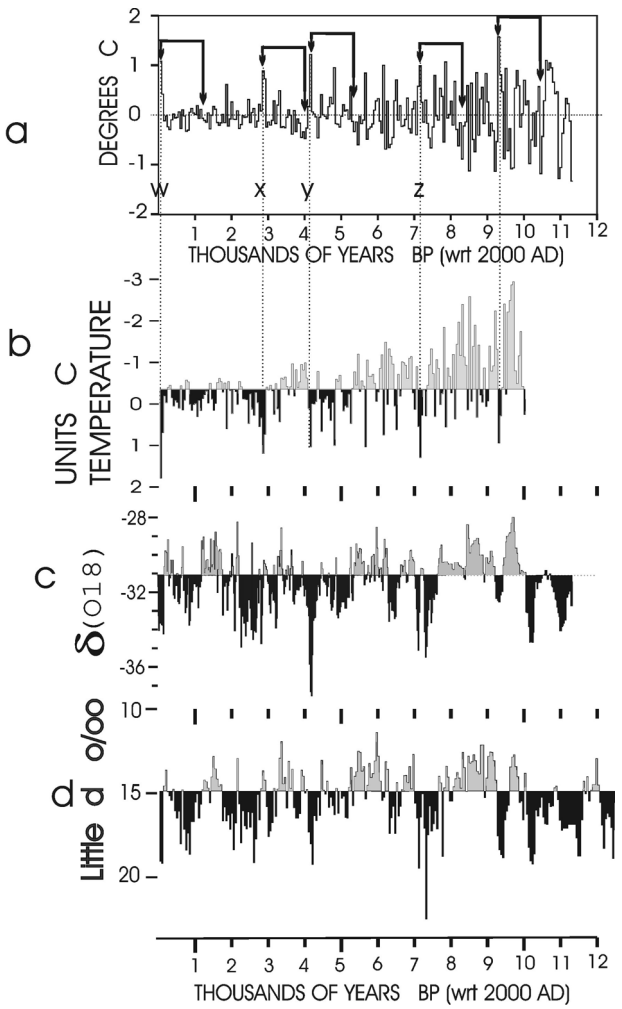


**Figure 8.** Generating the Mt Logan δ($^{18}$O) Holocene using the Agassiz melt layer record. (a) Agassiz melt-temperature residuals reproduced from Figure 6d. (b) The Agassiz temperature (melt) differenced with itself lagged 1150 years. It is proposed that this time series is a proxy for ($T_w - T_c$) which determines the strength of El Niño. (See text for details.) (c) Logan δ($^{18}$O). The correlation coefficient with (b) is −0.43, which is very significant. (d) Logan core little d (reversed axis) with bigger values downward suggests tropical sources supplies Logan moisture during times of vigorous El Niño/La Niña couples. Examples (w,x,y and z) of strong El Niño features are shown above and are due to pairs of high and low temperatures separated by 1150 years

the proposed Atlantic driver regions to the Pacific responder sites? Part of that answer is in the high-gain process suggested by Figure 3b. A driver series from the Atlantic could be smoothed by the ocean's diffusive GOC processes and have its details muted by the time it arrived in the tropical deep water. But an 'aggressive' ENSO-gain function like that in Figure 3b could regain some of the higher-frequency details of the muted lagged driver series.

The big Logan δ($^{18}$O) excursions are reproduced by the lagged difference series using the Arctic driver series, when there are large positive temperature anomalies paired with large negative temperature anomalies 1200 year earlier. Such pairs are indicated in Figure 8a along with the 'big El Niño episodes' that result (w, x, y and z). For example, the cooling event 8200 years ago (prevalent in the North Atlantic ice core records) paired with the warm period about 7100 years ago produces the 'z' El Niño feature. Also a warm–cold couple that is in the ice core records produces the large 'y' El Niño event 4200 years ago.

If the North Atlantic-sector temperatures from ice cores can generate the Logan δ($^{18}$O) and if it reflects the state of El Niño, then what can one surmise about the future? If a large ENSO amplitude is the result of $T_w - T_c$ being greater than 12 (see Figure 3b) and if the lag time is 1150 years, then our immediate future ENSO amplitude should be determined by a combination of our increasing SSTs in the tropical Pacific and the increasing temperatures in the North Atlantic that began 1150 years ago at the start of the so-called 'Medieval Warm Period' (MWP). If the deeper water warming from the high-latitude MWP exceeds the present warming in the tropical eastern Pacific SSTs, then one could expect to drift into the strong La Niña part of Sun's solution space (Figure 3b), whereas if the modern warming trend in the TEP exceeds that of the northern MWP then the most recent episode of strong El Niños should continue or even strengthen.

If the 1150-year lag is real, then what is happening today in the North Atlantic will re-visit our climate more than 1000 years into the future. If the present Pacific SST warming trend continues and combines with lagged bottom water temperatures from the 'Little Ice Age', it could make for some 'interesting' weather about nine centuries from now.

## References


Berger A and Loutre MF (1991) Insolation values for the climate of the last 10 million years. *Quaternary Science Reviews* 10: 297–317.

Broecker WS (1991) The great conveyor belt. *Oceanography* 4: 79–89.

Climate Research Unit (1992) *World Climate Disk*. Data from the Climatic Research Unit at the University of East Anglia, produced by Chadwyck-Healey.

D'Arrigo R, Cook E, Wilson R, Allen R and Mann M (2005) On the variability of ENSO over the past six centuries. *Geophysical Research Letters* 32(L03711): 1–4.

Field RD, Moore GWK, Holdsworth G and Schmidt GA (2010) A GCM-based analysis of circulation controls on δ($^{18}$O) in the southwest Yukon, Canada: Implications for climate reconstructions in the region. *Geophysical Research Letters* 37(L05706): doi: 10.1029/2009GL041408.

Fisher DA (1988) *The Summer Melt Record for the A87 and A84 Ice Cores: 1-year, 5-year and 50-year Means: Comparisons to Other Melt Records: Relationship Between Melt and δ($^{18}$O)*. Contract Report to Polar Continental Shelf Project. Scientific authority R.M. Koerner.

Fisher DA (1990) A zonally averaged stable-isotope model coupled to a regional variable-elevation stable isotope model. *Annals of Glaciology* 14: 65–71.

Fisher DA (1992) Stable isotope simulations using a regional isotope model coupled to a zonally averaged global model. *Cold Regions Science and Technology* 21: 61–77.

Fisher DA and Koerner RM (2003) Holocene ice-core climate history – A multi-variable approach. In: Mackay A, Battarbee R, Birks J and Oldfield F (eds) *Global Change in the Holocene*. New York: Oxford University Press, 281–293.

Fisher DA, Koerner RM and Reeh N (1995) Holocene climatic records from Agassiz Ice Cap, Ellesmere Island, NWT, Canada. *The Holocene* 5(1): 19–24.

Fisher DA, Osterberg E, Dyke A, Dahl-Jensen D, Demuth D, Zdanowicz C et al. (2008) The Mt. Logan Holocene–late Wisconsinan isotope record: Tropical Pacific–Yukon connections. *The Holocene* 18(5): 667–678.

Fisher DA, Wake C, Kreutz K, Yalcin K, Steig E, Mayewski P et al. (2004) Stable isotope records from Mount Logan and Eclipse Ice Cores and nearby Jellybean Lake; water cycle of the north Pacific over 2,000 years and over 5 vertical kilometres; sudden shifts and tropical connections. *Géographie physique et Quaternaire* 58(2–3): 337–352.

Fowler A (2008) ENSO history recorded in *Agathis australis* (kauri) tree-rings, Part B: 422 years of ENSO robustness. *International Journal of Climatology* 28(1): 21–35.

Froese D, Kuehn S, Fisher D, Zdanowicz C, Atkins C, Dunning H et al. (2010) Establishing independent age models for ice cores using tephrochronology. Abstract in International Field Conference on Tephrochronology, Volcanism and Human Activity. Kagoshima Japan, May 2010.

Gergis JL (2006) Reconstructing El Niño-Southern Oscillation; evidence from tree-ring, coral, ice and documentary paleoarchives, AD 1525–2002. Unpublished doctoral thesis, School of Biological, Earth and Environmental Sciences, University of New South Wales.


Downloaded from hol.sagepub.com at Masarykova Univerzita on April 4, 2013

Gergis JL and Fowler AM (2009) A history of ENSO events since 1525: Implications for future climate change. *Climate Change* 92: 343–387.

Holdsworth GH (2008a) A composite isotopic thermometer for snow. *Journal of Geophysical Research* 113(D08102): doi: 10.1029/2007JD008634.

Holdsworth GH (2008b) Interpreting $H_2O$ isotope variations in high-altitude ice cores using a cyclone model. *Journal of Geophysical Research* 113(D08103): doi: 10.1029/2007JD008639.

Holzer M and Primeau W (2006) The diffusive ocean conveyor. *Geophysical Research Letters* 33(L14618): doi: 10.1029/2006GL026232.

Johnsen SJ, Dansgaard W and White JW (1989) The origin of Arctic precipitation under present and glacial conditions. *Tellus* (Series B) 41: 452–468.

Kaufman DS, Schneider DP, McKay NP, Ammann CM, Bradley RS, Briffa KR et al. (2009) Recent warming reverses long-term Arctic cooling. *Science* 325: 1236.

Koerner RM and Fisher DA (1990) A record of Holocene summer climate from a Canadian High Arctic ice core. *Nature* 343: 630–631.

Laskar J (1990) The chaotic motion of the solar system: A numerical estimate of the size of the chaotic zones. *Icarus* 88: 266–291.

Mann ME, Bradley RS and Hughes MK (2000) Long-term variability in El Niño/Southern Oscillation and associated teleconnections. In: Diaz HF and Markgraf V (eds) *El Niño and the Southern Oscillation*. Cambridge: Cambridge University Press, 357–412.

Moore GWK, Alverson K and Holdsworth G (2005) Mount Logan ice core evidence for changes in the Hadley and Walker circulations following the end of the Little Ice Age. In: Bradley RA and Diaz H (eds) *The Hadley and Walker Circulations Following the End of the Little Ice Age*. New York: Springer, 371–395.

Moore GWK, Holdsworth G and Alverson K (2001) Extra-tropical response to ENSO as expressed in an ice core from the Saint Elias Mountain range. *Geophysical Research Letters* 28: 3457–3460.

Quinn WH and Neal VT (1992) The historical record of El Niño events. In: Bradley RS and Jones PD (eds) *Climate Since AD 1500.* London: Routledge, 623–648.

Quinn WH, Neal VT and Antunez de Mayolo SE (1987) El Niño occurrences over the past four and a half centuries. *Journal of Geophysical Research* 92: 14 449–14 461.

Stocker TF and Johnsen SJ (2003) A minimum thermodynamic model for the bipolar seesaw. *Paleooceanography* 18(4): 1087. doi: 10.1029/2003PA000920.

Sun D (2000) Global climate change and El Niño: A theoretical framework. In: Diaz HF and Markgraf V (eds) *El Niño and the Southern Oscillation*. Cambridge: Cambridge University Press, 443–464.

Thompson LG (1992) *Quelccaya Ice Core Database*. IGBP PAGES/World Data Center-A for Paleoclimatology Data Contribution Series # 92-008. NOAA/NGDC Paleoclimatology Program, Boulder CO, USA.

Thompson LG, Mosley-Thompson E and Arnao BM (1984) Major El Niño/Southern Oscillation events recorded in the stratigraphy of the tropical Quelccaya Ice Cap. *Science* 226(4670): 50–53.

Vinther BM, Buchardt SL, Clausen HB, Dahl-Jensen D, Johnsen SJ, Fisher DA et al. (2009) Holocene thinning of the Greenland ice sheet. *Nature* 461: 385–388.

Vinther BM, Clausen HB, Johnsen SJ, Fisher DA, Koerner RM, Andersen KK et al. (2008) Synchronizing ice cores from the Renland and Agassiz ice caps to the Greenland ice core chronology. *Journal of Geophysical Research* 113(D08115): doi: 10.1029/2007JD009143.

Zielinski GA, Mayewski PA, Meeker LD, Grönvold K, Germani MS, Whitlow S et al. (1997) Volcanic aerosol records and tephrochronology of the Summit, Greenland, ice cores. *Journal of Geophysical Research* 102(C12): 26 625–26 640.

Downloaded from hol.sagepub.com at Masarykova Univerzita on April 4, 2013